Abdominal Lymphadenopathy: Spectrum of CT Findings[1]

David M. Einstein, MD
Anne A. Singer, MD
William A. Chilcote, MD
Robert K. Desai, MD

Many malignant processes cause abdominal lymphadenopathy, and computed tomography (CT) has become the primary modality for its detection. Diagnosis of lymphadenopathy is facilitated by optimal imaging techniques and a knowledge of the various nodal chains, their complex interconnections, and preferential pathways of spread. Optimal techniques include imaging after oral administration of adequate amounts of barium suspension and dynamic scanning after intravenous administration of contrast material with an infusion pump. Although such techniques help prevent misdiagnoses due to normal and anomalous vascular structures, other benign diseases can mimic the CT appearance of malignant lymphadenopathy. The authors emphasize a regional approach for the diagnosis of lymphadenopathy, according to the groupings of retrocrural, retroperitoneal, gastrohepatic ligament, porta hepatis, celiac and superior mesenteric artery, pancreaticoduodenal, perisplenic, mesenteric, and pelvic lymph nodes. Lymphadenopathy is defined as retrocrural nodes greater than 6 mm in short axis, upper abdominal nodes greater than 10 mm, and pelvic nodes greater than 15 mm.

■ INTRODUCTION

The network of lymph nodes in the body plays an important role in the immune system. It provides protection against organisms, particulate matter, and neoplastic cells, removing them from the lymphatic circulation by phagocytosis and destroying them by cell- and antibody-mediated immune processes. Lymph nodes are also involved in the production of B and T lymphocytes and antibody-producing plasma cells. The adult body contains some 400–500 lymph nodes, with approximately 230 nodes in the abdomen and pelvis.

Index terms: Abdomen, CT, 70.1211 • Abdomen, neoplasms, 70.30 • Lymphatic system, CT • Lymphatic system, neoplasms • Pelvis, CT, 80.1211 • Pelvis, neoplasms, 80.30

RadioGraphics 1991; 11:457–472

[1] From the Department of Diagnostic Radiology, Cleveland Clinic Foundation, 9500 Euclid Ave, Cleveland, OH 44195. From the 1990 RSNA scientific assembly. Received January 11, 1991; revision requested February 12 and received February 20; accepted February 21. **Address reprint requests to** D.M.E.

© RSNA, 1991

Many diseases, both neoplastic and inflammatory, result in abdominal lymphadenopathy. Because there is a complex pattern of intercommunications between regional groups of lymph nodes, it is not unusual for lymphadenopathy to involve several contiguous or even widely separated nodal chains.

Lymphangiography was the primary method of evaluating the lymphatic system for metastatic disease before the development of computed tomography (CT). Although lymphangiography accurately displays the internal architecture of the pelvic and paraaortic nodes, it is invasive, time-consuming, and difficult to perform. Furthermore, many lymph node groups, particularly the portal, celiac, mesenteric, and retrocrural, are not opacified. With CT, the entire abdominopelvic lymphatic system can be evaluated, as can the solid organs and adjacent bone structures, providing a more extensive evaluation of the neoplastic process (1). This information is vital for accurate staging, prognosis, choice of proper therapy, and follow-up of oncology patients. CT has thus become the initial procedure of choice in the detection of abdominal lymphadenopathy.

In this article, we present a spectrum of CT findings in abdominal lymphadenopathy. As a basis for the interpretation of abdominal CT scans, we have empirically grouped the abdominal and pelvic lymph nodes into nine major nodal groups: retrocrural, retroperitoneal, gastrohepatic ligament, porta hepatis, celiac and superior mesenteric artery, pancreaticoduodenal, perisplenic, mesenteric, and pelvic. In addition, we describe dynamic CT techniques appropriate for diagnosis of abdominal lymphadenopathy, present currently recommended size criteria for enlarged nodes, discuss pitfalls of CT diagnosis including sources of false-positive and false-negative results, and describe patterns of preferential spread of many common malignant neoplasms. Because the lymphadenopathy produced by neoplastic conditions tends to be of greater magnitude than that due to benign conditions, the examples presented herein are predominantly neoplastic in pathogenesis.

■ CT IN THE DIAGNOSIS OF LYMPHADENOPATHY

• CT Technique

The oral administration of adequate amounts of contrast material is essential to avoid misinterpretation of unopacified loops of bowel as enlarged lymph nodes, particularly in the retroperitoneum and mesentery (1). Our current regimen is to administer 500 mL of a 1.2% weight-to-weight ratio dilute barium suspension (Readi-CAT; E-Z-Em, Westbury, NY) at 2 hours and at 1 hour before scanning. A final 250 mL of contrast material is given while the patient is on the CT couch immediately before scanning is initiated.

Our routine protocol for intravenous administration of contrast material is to use an infusion pump to inject a total of 150 mL of iohexol 240 (Omnipaque 240; Winthrop Pharmaceuticals, New York), given as a bolus of 1.6 mL/sec for 100 mL and infused at a rate of 0.2 mL/sec for the remaining 50 mL. Image acquisition is initiated 30–45 seconds after the injection is begun and is continued dynamically as quickly as the given CT scanner will allow. This technique provides good vascular opacification throughout the examination, which allows differentiation of enlarged nodes from adjacent normal vascular structures; this can be particularly useful in interpreting the pelvic lymph nodes. Optimal enhancement of the pelvic veins usually occurs at 3 minutes after initiation of the bolus injection of contrast material and continues until at least 7 minutes (2).

When problems of interpretation arise, it is often helpful to obtain delayed scans through the area of interest after additional contrast material has been administered orally or to obtain a one-level dynamic scan after an intravenous injection of a small bolus of

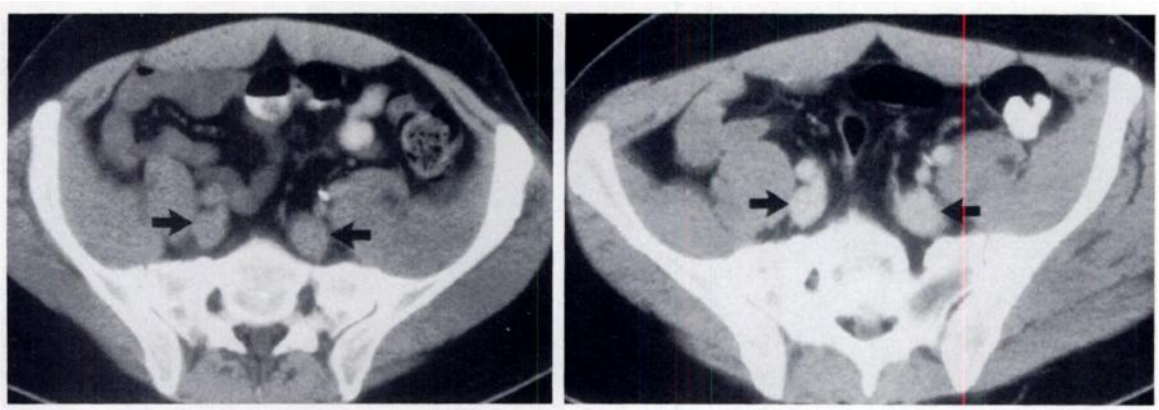

a. b.

Figure 1. **(a)** Dynamic CT scan shows equivocal pelvic nodal enlargement (arrows). **(b)** Dynamic CT scan obtained at the same level after bolus injection of contrast material demonstrates that the suspected nodes are really prominent vascular structures (arrows).

contrast material (Fig 1). Obtaining thinner sections to obviate artifacts due to partial volume averaging or changing patient position, which may alter the orientation of bowel loops, may also be useful (3).

• Criteria of Abnormality

State-of-the-art CT scanners currently offer excellent contrast and spatial resolution, often resulting in visualization of normal retroperitoneal and mesenteric lymph nodes. Normal pelvic and perivisceral nodes are less routinely seen due to the multiple small adjacent vessels. The sole criterion used in determining if a lymph node is abnormal is enlarged size; CT is unable to display abnormal architecture in a normal-sized node (4,5). This is the most significant shortcoming of the technique and a source of the majority of false-negative results from CT examinations. Lymphangiography may thus still be indicated in patients with selected malignant diseases that cause only mild lymphadenopathy, such as Hodgkin disease and seminoma, if initial staging at CT examination is negative (3).

Additional sources of false-negative results are artifacts due to partial volume averaging and variable respiratory excursions. These artifacts are overcome in clinical practice by obtaining contiguous 8- or 10-mm sections, fast scanning, and coaching the patient in breathing techniques.

Early in the development of CT, investigators advocated size thresholds of 1.5–2 cm for abnormally enlarged lymph nodes (5–7). With refinements in scanner technology leading to improved resolution, less liberal size criteria have been suggested. In these current guidelines for the various anatomic regions, short-axis measurements should be used to minimize errors due to node orientation. Retrocrural and porta hepatis nodes should not exceed 6 mm, while the upper limit of normal for gastrohepatic ligament nodes is 8 mm (4,8–10). Retroperitoneal, celiac axis, and mesenteric nodes greater than 10 mm in size are considered abnormal, but multiple, slightly smaller (8–10 mm) nodes in these regions should be viewed with suspicion (8,9). Because of the greater degree of difficulty in interpreting the pelvic lymphatic chains, primarily related to the multiple neighboring vascular structures, only those pelvic nodes exceeding 15 mm should be interpreted as enlarged (4,8). Although 3 mm has been recommended as a size threshold for perirectal lymphadenopathy, the reported sensitivity in detecting histologically proved nodal involvement in rectal carcinoma is only 27% (11).

Although CT is unable to display internal nodal architecture accurately, enlarged

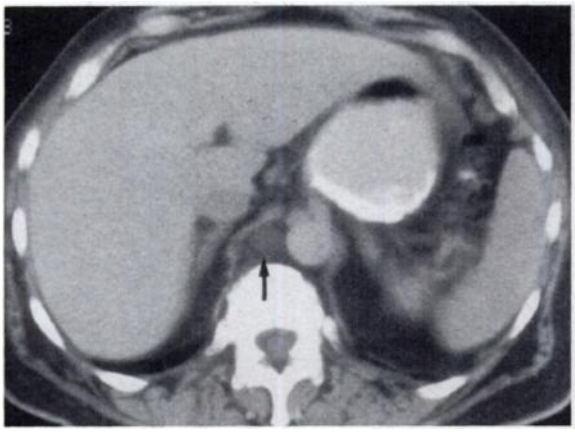

2.

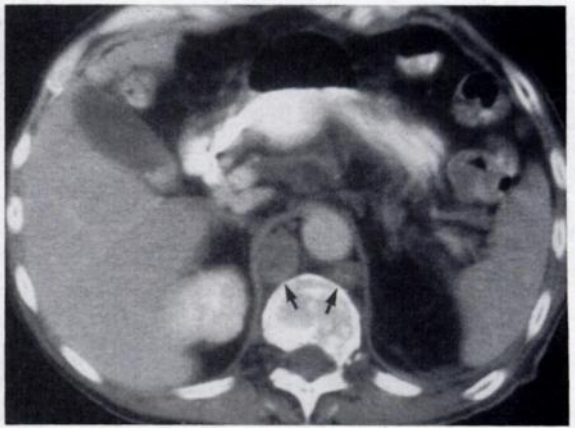

3.

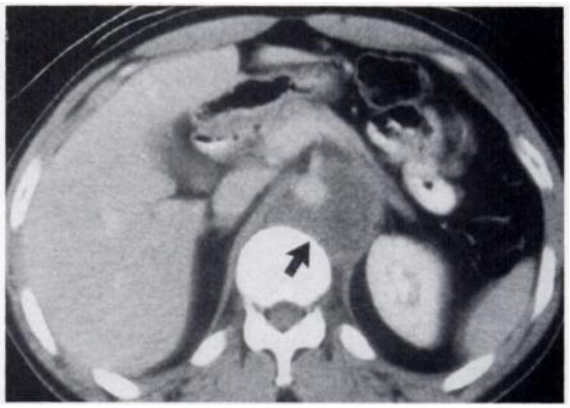

4.

Figures 2–4. (2) CT scan of a patient with peptic ulcer disease but no known underlying malignant process demonstrates a 1.2-cm retrocrural node (arrow), thought to be enlarged due to inflammation or reaction. (3) CT scan of a 61-year-old man with chronic lymphocytic leukemia shows two large well-defined retrocrural nodes (arrows). (4) CT scan reveals confluent retrocrural lymphadenopathy (arrow) in a 38-year-old patient with lymphoma.

nodes may also demonstrate CT attenuation values that may help in constructing a differential diagnosis. Calcified enlarged nodes may be postinflammatory or can be seen in mucinous carcinomas, sarcomas, and treated lymphomas. Although nodal metastases from nonseminomatous testicular tumors are classically described as being low in attenuation, several neoplastic and benign entities such as epidermoid genitourinary carcinomas, lymphoma, Whipple disease, and tuberculosis may also have this appearance (4).

• False-Positive Findings and Pitfalls in the Diagnosis of Lymphadenopathy

There are several normal structures, anatomic variants, and other disease processes that may complicate evaluation of the abdominal lymph nodes. Problems relating to unopacified bowel and prominent normal vascular structures such as gonadal veins and iliac vessels can be avoided with use of proper oral and intravenous administration of contrast material. Vascular anomalies including left-sided or duplicated inferior vena cava and varices resulting from portal hypertension can be recognized by their enhancement pattern. A papillary process of the caudate lobe or a bulbous, scalloped diaphragmatic crus may simulate lymphadenopathy in the portacaval space or retrocrural region, respectively, while an accessory spleen or normal ovarian tissue may also lead to confusion (3,12,13).

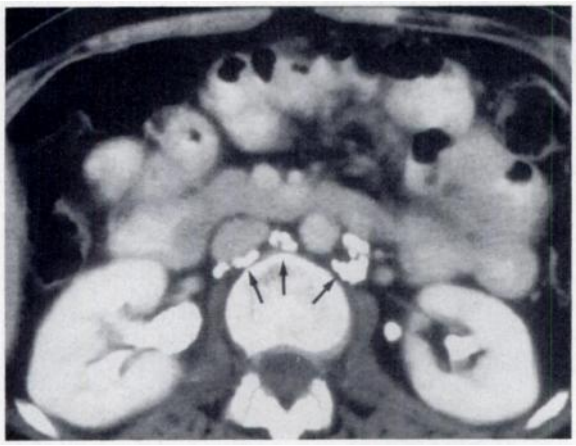

Figure 5. CT scan obtained subsequent to lymphangiography shows multiple, opacified, normal-sized retroperitoneal nodes (arrows).

Perhaps 5%–10% of cases of abdominal lymphadenopathy detected with CT will be related to benign processes rather than malignant infiltration (14). Sarcoidosis, tuberculosis, mastocytosis, Crohn disease, Whipple disease, and nontropical sprue all may cause nodal enlargement (3,14). Unfortunately, there are no distinctive features with which to distinguish benign from malignant lymphadenopathy, and individual nodes greater than 2 cm in size and even confluent node mantles may be seen in benign diseases (14). It has also been observed that nodes previously involved with malignant processes may remain enlarged after chemotherapy or radiation therapy, even when the patient is free of tumor (4).

Finally, there are several unrelated diseases that may mimic lymphadenopathy, particularly in the retroperitoneal and mesenteric regions. Retroperitoneal fibrosis, either primary or perianeurysmal, may closely simulate retroperitoneal lymphadenopathy but tends to have a more squared-off appearance and often enhances with intravenous contrast material (1,3). Primary retroperitoneal mesenchymal tumors and mesenteric desmoids may also lead to difficulties in differential diagnosis.

■ REGIONAL PATTERNS OF LYMPHADENOPATHY

• Retrocrural Nodes

The retrocrural space connects the posterior mediastinum to the retroperitoneum and contains the aorta, thoracic duct, azygos vein, hemiazygos vein and retrocrural lymph nodes. Lymphatics from the diaphragm, posterior mediastinum, and upper lumbar region drain directly to the retrocrural nodes, while the thoracic duct is the final lymphatic pathway from the entire pelvis, retroperitoneum, and peritoneal cavity.

Diseases originating above or below the diaphragm can communicate via the retrocrural space (13). Although lung carcinoma, mesothelioma, and lymphoma are the most common malignant diseases to involve this nodal group, other processes, both benign and malignant, may cause retrocrural lymphadenopathy (Figs 2–4). Retrocrural nodes are considered to be enlarged when they exceed 6 mm in size.

• Retroperitoneal Nodes

These nodes are present in a perivascular distribution about the aorta and inferior vena cava and are grouped into the periaortic, pericaval, and interaortocaval chains (Fig 5). Degrees of lymphadenopathy range from mildly enlarged discrete nodes to large man-

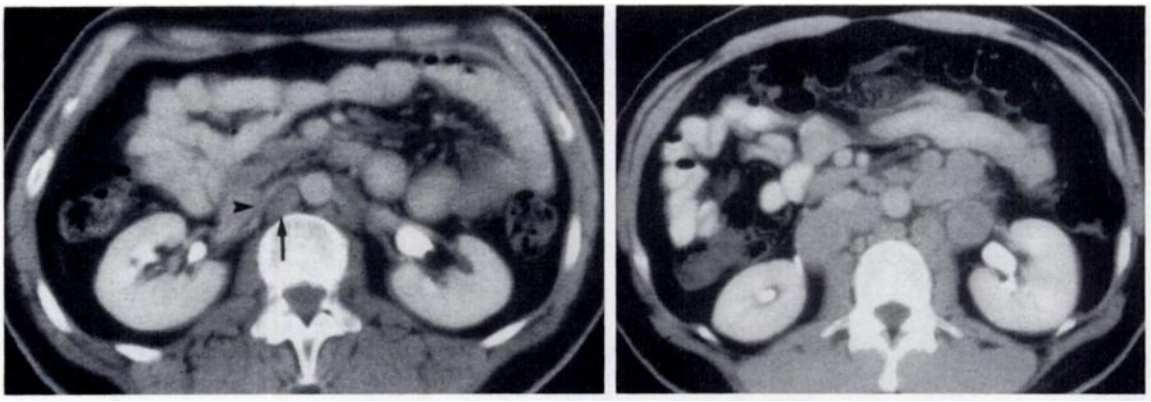

6. 7.

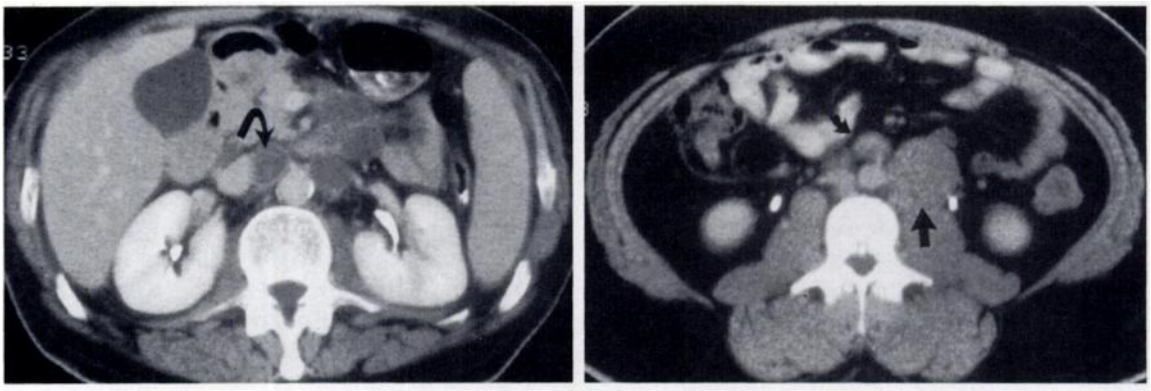

8. 9.

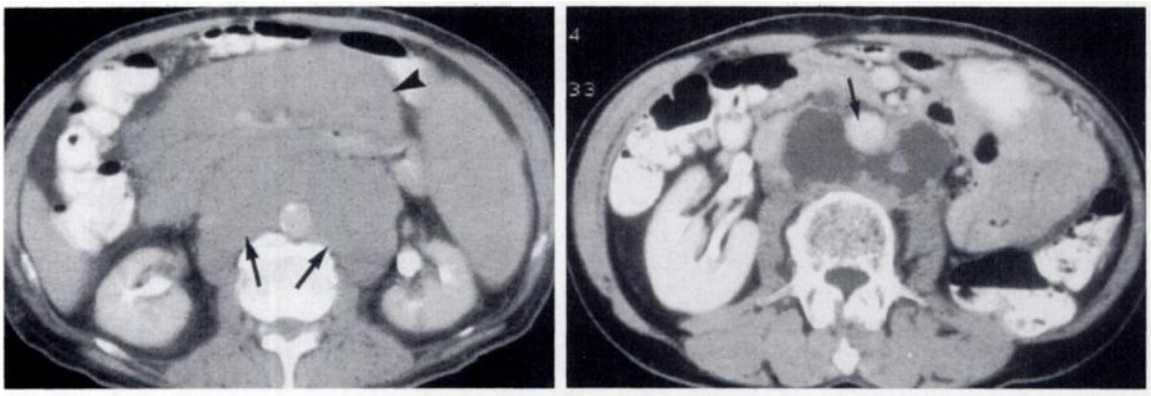

10. 11.

Figures 6–11. **(6)** CT scan demonstrates mild retroperitoneal lymphadenopathy (arrow) displacing the right renal artery (arrowhead) anteriorly. **(7)** CT scan shows multiple, discrete, enlarged retroperitoneal nodes in a 40-year-old man with lymphoma. **(8)** CT scan of a patient with large cell carcinoma of the lung shows low-attenuation retroperitoneal lymph nodes (arrow). **(9)** CT scan obtained for staging of malignant testicular teratoma reveals characteristic retroperitoneal lymphadenopathy (arrows) below the renal hilum. **(10)** CT scan of a patient with chronic lymphocytic leukemia shows a large mantle of confluent retroperitoneal lymphadenopathy (arrows). Note also extensive mesenteric lymphadenopathy (arrowhead). **(11)** CT scan reveals necrotic lymph nodes surrounding and anteriorly displacing a brightly enhanced aorta (arrow) in a 72-year-old man with transitional cell carcinoma of the bladder.

tles of confluent adenopathy, which may elevate the great vessels (Figs 6–11). Retroperitoneal nodes greater than 10 mm in size are considered to be enlarged, although if numerous 8–10-mm nodes are present, lymphadenopathy should be suspected.

The pelvic nodal chains drain directly into the retroperitoneal nodal system, and there are numerous interconnections with the celiac and mesenteric nodal systems as well

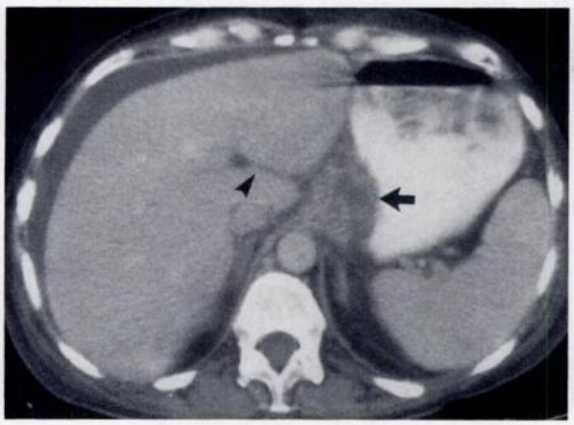

12.

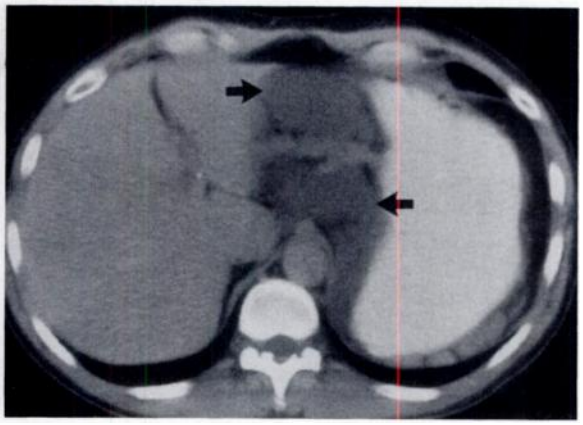

13.

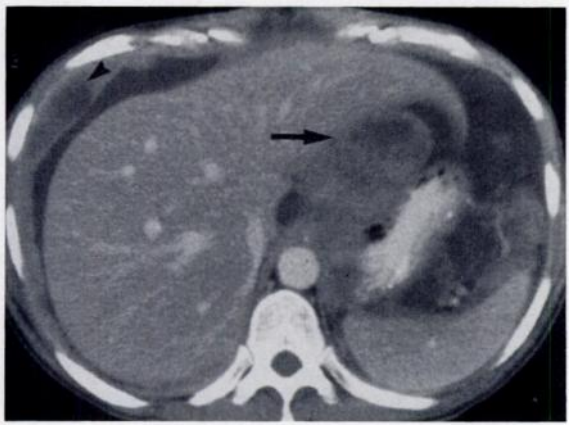

14.

Figures 12–14. **(12)** CT scan of a 43-year-old patient with lymphoma demonstrates gastrohepatic ligament lymphadenopathy (arrow) adjacent to the fissure of the ligamentum venosum (arrowhead). **(13)** CT scan demonstrates gastrohepatic ligament lymphadenopathy (arrows) surrounding enhanced vascular structures in a 62-year-old man with rectal carcinoma. **(14)** CT scan of a 47-year-old patient with malignant melanoma reveals malignant ascites, peritoneal implants (arrowhead), and partially necrotic gastrohepatic ligament nodes (arrow).

(15). Thus, virtually any intraabdominal or pelvic neoplasm may cause retroperitoneal lymphadenopathy, but the most common are lymphoma and renal cell, testicular, cervical, and prostatic carcinomas, the latter two after first involving the pelvic nodes. Thoracic neoplasms may also spread here via retrograde flow through the retrocrural nodes.

• Gastrohepatic Ligament Nodes

The gastrohepatic ligament is the superior portion of the lesser omentum and contains the left gastric artery, coronary vein, and left gastric nodes. The gastrohepatic ligament suspends the stomach from the liver and blends into the fissure of the ligamentum venosum; thus, it can be identified on CT sections containing this landmark (Fig 12) (10). Drainage from the gastrohepatic ligament nodes is to the celiac nodal group.

Carcinoma of the lesser curvature of the stomach and distal esophagus often causes regional adenopathy in the gastrohepatic ligament nodal group. These nodes may also be enlarged by disseminated lymphoma, retrograde spread from celiac nodes involved by carcinoma of the pancreas, and metastatic spread from a variety of distant primary malignant processes, including melanoma and carcinoma of the colon and breast (Figs 13, 14). Gastrohepatic ligament nodes are considered to be enlarged when they exceed 8 mm in size. Potential diagnostic pitfalls include mistaking coronary varices or the upper margin of the pancreas and transverse colon for mild lymphadenopathy (10).

15.

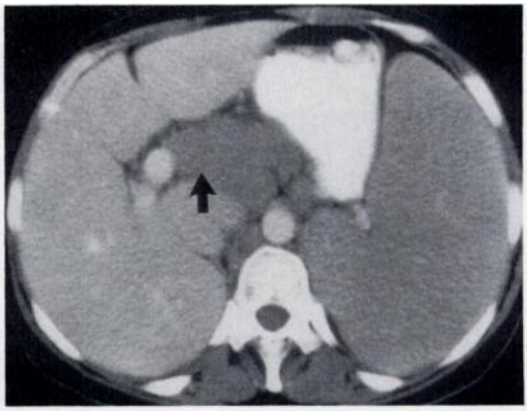

16.

17a.

17b.

Figures 15–17. **(15)** CT scan of a patient with primary biliary cirrhosis reveals nonconfluent mild portal lymphadenopathy (arrows) surrounding the enhanced portal vein. **(16)** CT scan of a 57-year-old patient with lymphoma shows confluent portal lymphadenopathy (arrow). **(17)** CT scans of the liver in a patient with lymphoma reveals mild portal lymphadenopathy (arrow in **a**) resulting in periportal lymphedema (arrow in **b**).

• Porta Hepatis Nodes

Portal nodes lie within the porta hepatis, extending down the hepatoduodenal ligament and interconnecting with the gastrohepatic ligament nodes. Central drainage is to the celiac nodes (15,16). The portal nodes lie anterior and posterior to the portal vein and, when enlarged, may completely surround and even obliterate this structure. Hence, adequate enhancement with intravenous contrast material is essential for diagnosis, particularly when only mild lymphadenopathy is present (Fig 15) (17). Portal nodes are abnormal if greater than 6 mm in size.

Adenopathy of the portal nodes not uncommonly causes high extrahepatic biliary obstruction. Many primary neoplasms spread to the portal nodes, including those arising in the gallbladder and biliary tree, liver, stomach, pancreas, colon, lung, and breast. Lymphoma also frequently involves these nodes when abdominal dissemination is present (Figs 16, 17). Because the portal nodes are in direct continuity with the intrahepatic lymphatic system, lymphadenopathy in this region is often associated with liver metastases (17).

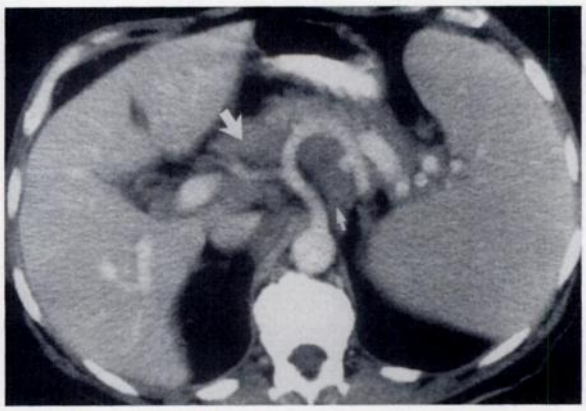

18.

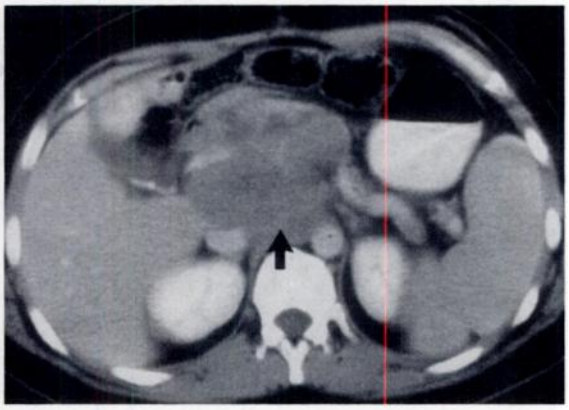

19.

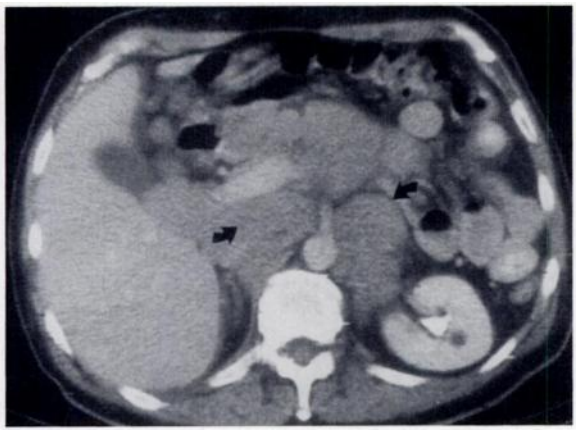

20.

Figures 18–20. **(18)** On dynamic CT scan with good vascular opacification, branches of the celiac axis can be clearly distinguished from the surrounding adenopathy (arrows). **(19)** CT scan of a 33-year-old man with widely disseminated colon carcinoma reveals massive celiac lymphadenopathy (arrow). **(20)** CT scan clearly shows nodes (arrows) surrounding the origin of the superior mesenteric artery in a 62-year-old man with lymphoma.

• Celiac and Superior Mesenteric Artery Nodes

The celiac and superior mesenteric artery nodes, along with the nodes at the base of the inferior mesenteric artery, are termed preaortic nodes and have interconnections with the retroperitoneal periaortic nodes (15). Because the inferior mesenteric artery is not often visualized as a discrete structure on CT scans, nodes here are difficult to distinguish from retroperitoneal nodes. The celiac and superior mesenteric artery nodes are clustered around the origins of their respective vessels and are easily distinguished, however (Figs 18–20). These two groups are the terminal nodes of the gastrointestinal tract from the ligament of Treitz to the splenic flexure, receiving lymph from the mesenteric, iliocolic, and colic nodal chains. Portions of the pancreas also drain to this group of nodes. Interconnections to the portal and splenic nodal chains also exist; thus, virtually any intraabdominal neoplasm may cause adenopathy of the celiac and superior mesenteric artery nodes (15). These nodes are considered abnormal when they are greater than 10 mm in size. Enlargement of other more primary nodal sites may point toward the initial organ of involvement.

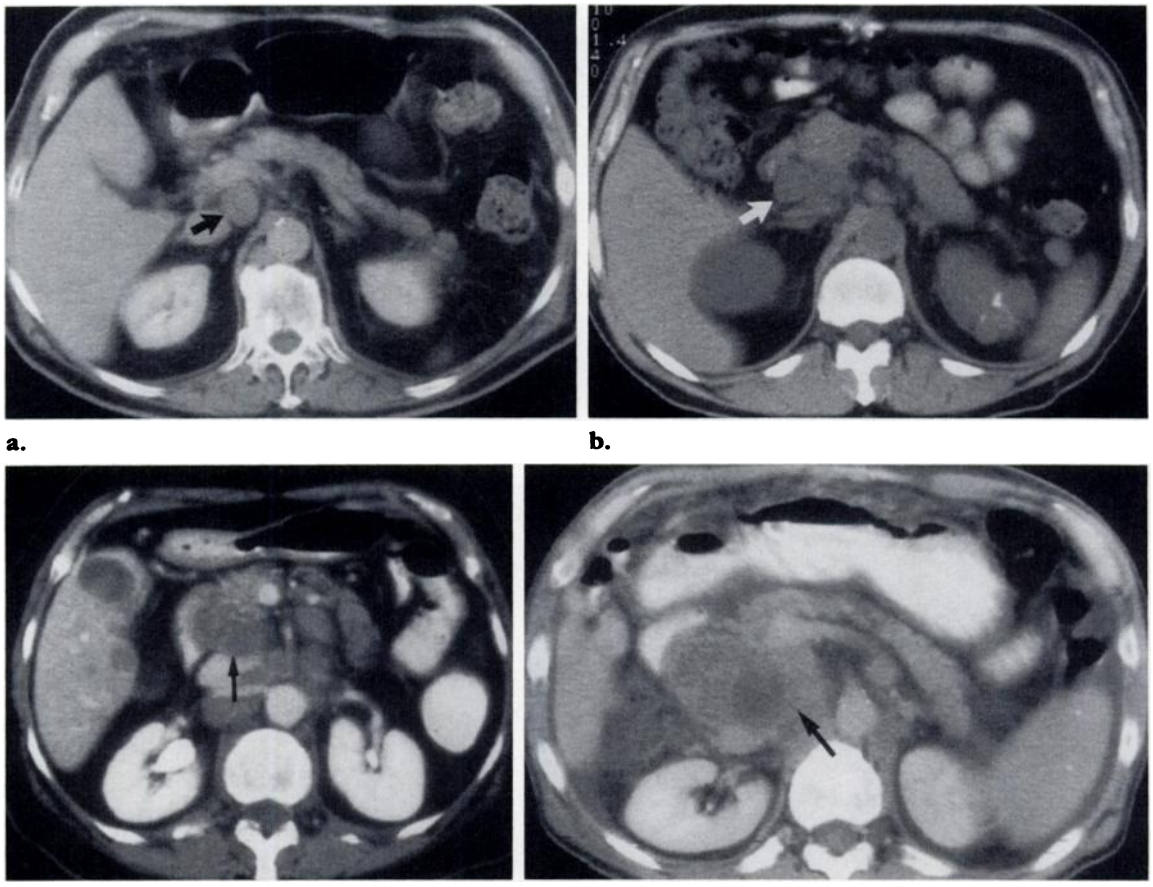

Figure 21. Spectrum of pancreaticoduodenal lymphadenopathy as noted on CT scans. **(a)** Solitary, enlarged pancreaticoduodenal node (arrow) is clearly separable from adjacent structures. Retrocrural lymphadenopathy is also present. **(b)** Enlarged nodes (arrow) are seen posterior to the pancreatic head, medial to the duodenum, and anterior to the inferior vena cava. Note the superior portion of a calcified renal cell carcinoma of the left kidney. **(c)** There is no clear cleavage plane between the lymphadenopathy (arrow) and the pancreatic head and uncinate process. Enlarged retroperitoneal and superior mesenteric artery lymph nodes, as well as hepatic metastases, are also present. **(d)** CT scan shows massive pancreaticoduodenal lymphadenopathy (arrow) causing an extrinsic pressure effect on the duodenum due to metastatic malignant fibrous histiocytoma.

• Pancreaticoduodenal Nodes

Pancreaticoduodenal nodes lie between the duodenal sweep and pancreatic head, anterior to the inferior vena cava (Fig 21a, 21b). They are often grouped with the pericaval and superior mesenteric artery nodes into a category of peripancreatic nodes. When enlarged, they may cause distal extrahepatic biliary obstruction. If confluent nodal enlargement occurs, it may be difficult to differentiate from a pancreatic head carcinoma unless a clear cleavage plane exists (Fig 21c, 21d). Sonography may occasionally be helpful in making this differentiation. Pancreaticoduodenal nodes may communicate with nodes in the porta hepatis via lymphatics in the hepatoduodenal ligament, and thus lymphadenopathy of the pancreaticoduodenal nodes commonly coexists with hepatic parenchymal metastases. Lymphoma and carcinoma of the pancreatic head, colon, stomach, lung, and breast are the most common malignant processes to involve these nodes (18). Nodes in this location exceeding 10 mm in size are considered enlarged.

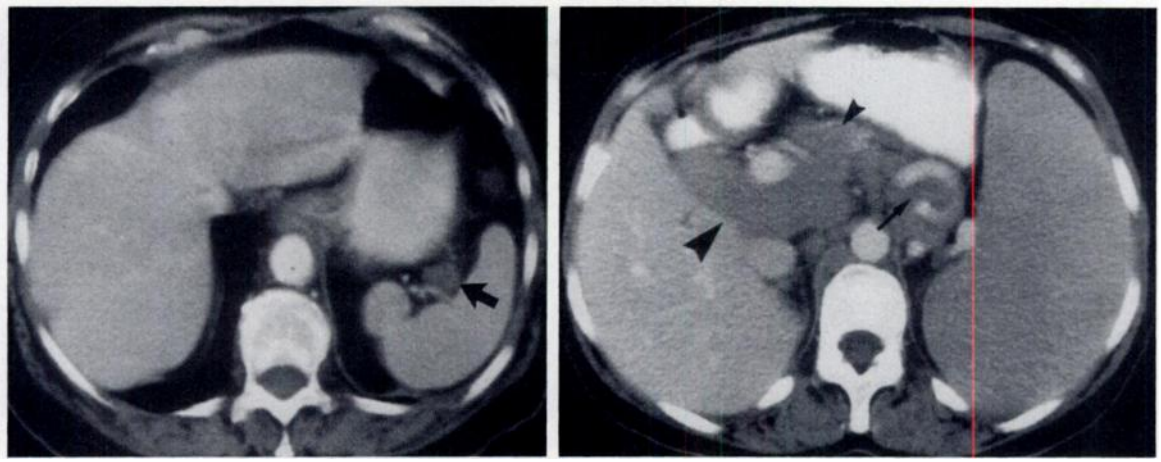

a. b.

Figure 22. **(a)** CT scan of a patient with lymphoma demonstrates a solitary enlarged splenic hilum node (arrow). **(b)** CT scan of another patient with lymphoma demonstrates extensive lymphadenopathy surrounding the splenic artery (arrow). Portal lymphadenopathy extending along the hepatoduodenal ligament (arrowheads) is also seen.

• Perisplenic Nodes

Perisplenic lymph nodes lie in the splenic hilum and drain the spleen, greater curvature of the stomach, and tail of the pancreas. Eventual drainage is to the celiac group via the pancreaticosplenic chain of nodes, which runs along the extent of the pancreas. Lymphoma and primary neoplasms of the pancreas, colon, stomach, lung, and breast commonly enlarge the perisplenic nodes (Fig 22) (15). The upper limit of normal for these nodes is 10 mm.

• Mesenteric Nodes

The small bowel mesentery contains a large number of nodes that accompany the branches of the superior mesenteric artery and vein. Multiple nodes are also present more distally, adjacent to the bowel wall. Eventual lymphatic drainage is to the superior mesenteric artery nodes at the base of the mesentery and from there, to the retroperitoneal nodes (15). Non-Hodgkin lymphoma, leukemia, small bowel neoplasms, ovarian carcinoma, and carcinoma of the right and transverse colon are common causes of mesenteric lymphadenopathy, with metastases from lung and breast carcinoma also occasionally seen (19,20). Mesenteric lymphade-

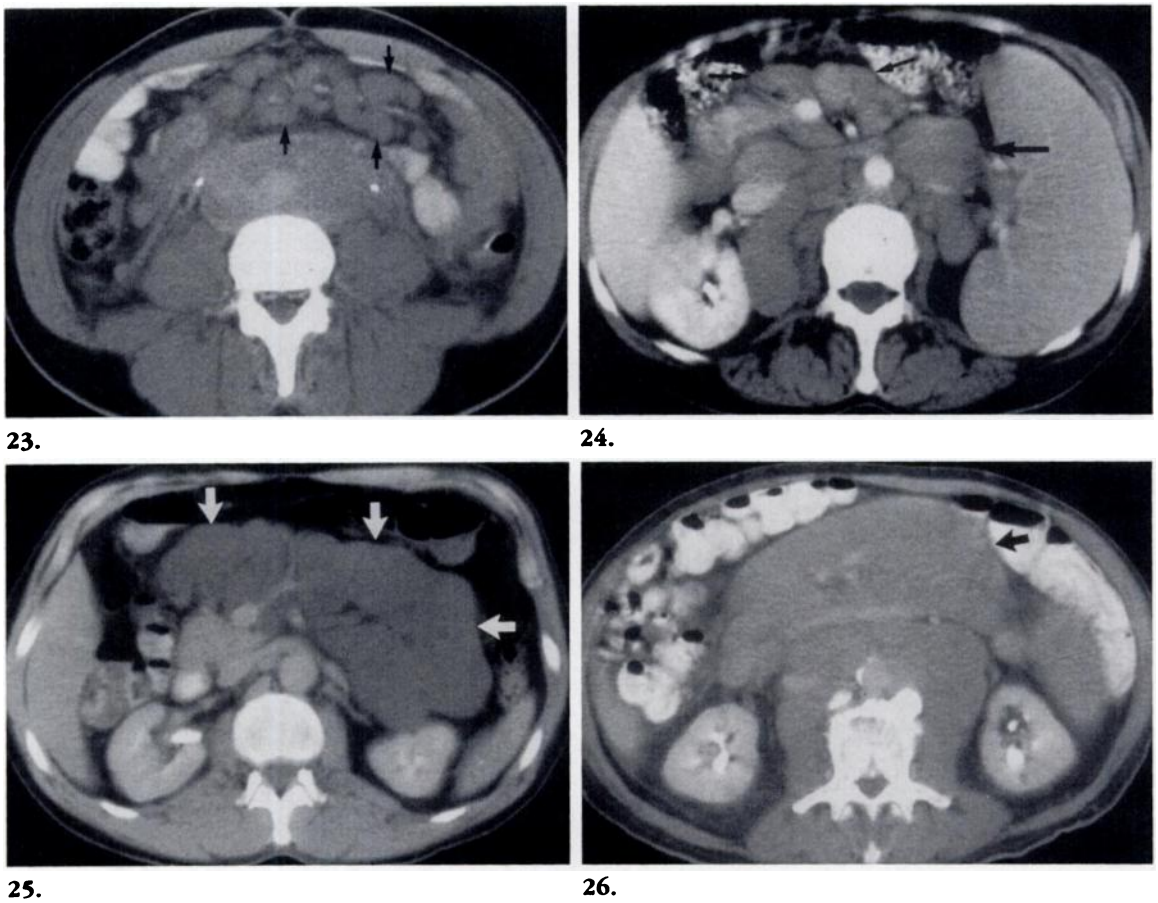

Figures 23–26. **(23)** CT scan of a patient with lymphoma demonstrates multiple, mildly enlarged mesenteric nodes (arrows) surrounding an enhanced branch of the superior mesenteric artery. A confluent mantle of retroperitoneal lymphadenopathy is also present. **(24)** CT scan of a 57-year-old woman with lymphoma shows extensive mesenteric lymphadenopathy (arrows). **(25)** CT scan of a patient with rectal carcinoma reveals massive lymphadenopathy (arrows) in the root of the mesentery. **(26)** CT scan of a patient with chronic lymphocytic leukemia (same patient as in Fig 10) demonstrates confluent lymphadenopathy (arrow) surrounding the superior mesenteric vein and artery (the "sandwich sign").

nopathy can vary from small discrete nodules (greater than 10 mm in size) to large masses of adenopathy sandwiching normal vessels and fat (Figs 23–26) (21).

• Pelvic Nodes

Pelvic nodes constitute an extensive nodal group, clustered along the common, external, and internal iliac vessels. At the level of the inferior sacroiliac joint, the external iliac vessels and nodes diverge anteriorly, lying adjacent to the psoas muscle, with the internal iliac vessels and nodes assuming a more posterior location (Figs 27–29) (1,5,7). The pelvic nodes have traditionally been considered more difficult to interpret than the retroperitoneal nodes, due predominantly to the variable diameter, location, and transaxial orientation of the iliac vessels (1,7). Hence, the size criterion of abnormality for pelvic nodes is greater than that used in the

27a.

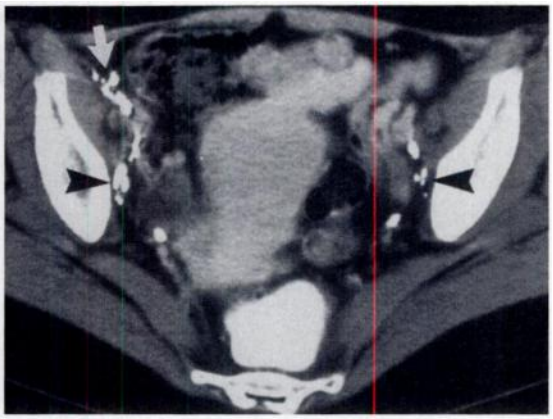

27b.

28a.

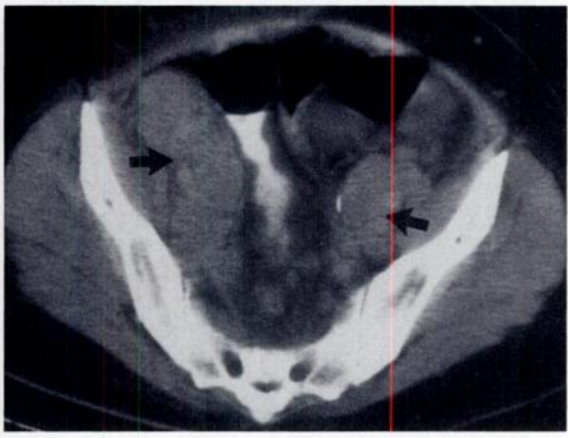

28b.

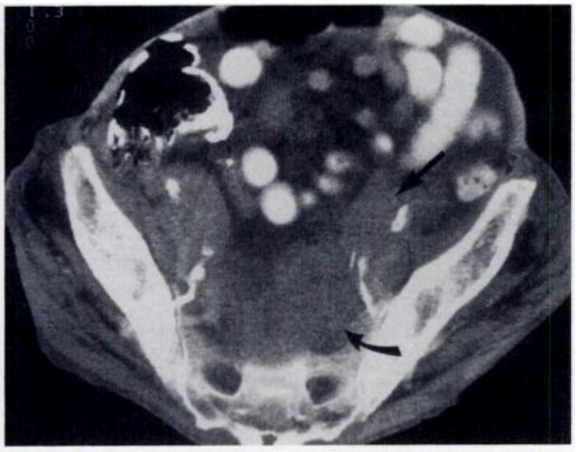

29.

Figures 27–29. **(27)** CT scans of normal-sized pelvic lymph nodes opacified due to prior lymphangiography. Common iliac (arrows in **a**), external iliac (arrow in **b**), and obturator (arrowheads in **b**) lymph nodes are seen. **(28)** CT scans of a 46-year-old woman with lymphoma demonstrate extensive bilateral common iliac lymphadenopathy (arrows in **a**) and asymmetric external iliac nodal enlargement (arrows in **b**). **(29)** CT scan of a patient with chronic lymphocytic leukemia demonstrates external (straight arrow) and internal (curved arrow) iliac lymphadenopathy clearly discernible from surrounding calcified iliac artery branches.

retroperitoneal region (15 mm vs 10 mm). Any asymmetry in the areas of the iliac vessels may also be an indication of early lymphadenopathy (Fig 30).

The pelvic nodes have extensive interconnections to the inguinal, lower extremity, and retroperitoneal nodal chains. Carcinomas of the bladder, prostate, cervix, and uterus initially spread to the pelvic nodes, as may carcinoma of the anorectal region after first involving nodes in the pararectal space. Testicular, ovarian, and fallopian tube malignant processes spread first to the retroperitoneal nodes (Fig 9) but may involve the pelvic nodes via retrograde spread. Disseminated lymphoma is another frequent cause of pelvic lymphadenopathy.

The obturator node is especially important to evaluate, since it is the first point of spread from carcinomas of the prostate, bladder, and cervix. It is classified as part of the external iliac chain and is related to the obturator vessels and nerves posterior to the external iliac vessels (7). It is best seen on CT images obtained 2–3 cm above the acetabulum and is located along the medial wall of the iliac bone, which at this level has a teardrop configuration (Fig 31) (3,7).

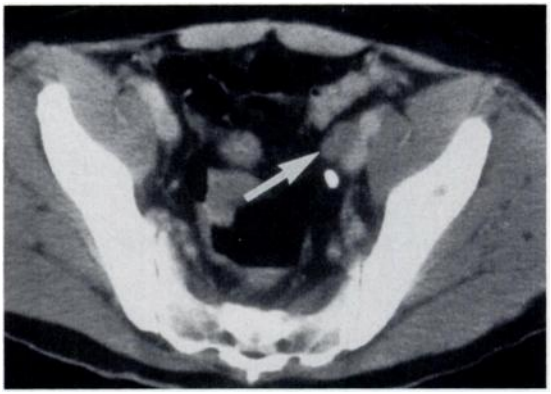

a.

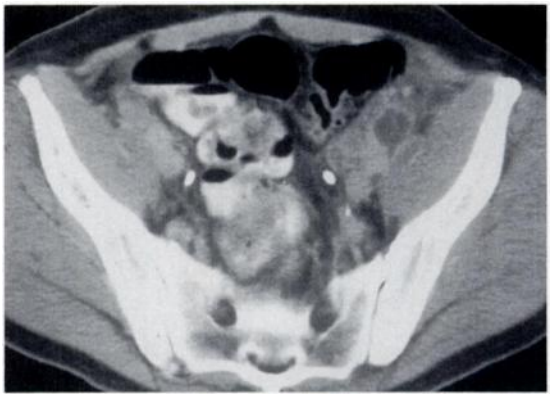

b.

Figure 30. **(a)** CT scan of a 55-year-old man shows subtle, asymmetric nodules of soft-tissue attenuation (arrow) medial to well-opacified vessels, findings indicative of early left external iliac lymphadenopathy. **(b)** On CT scan obtained 3 months later, the nodes have enlarged further and become necrotic. The patient proved to have metastatic renal cell carcinoma.

■ PATTERNS OF TUMOR SPREAD

Malignant neoplasms spread first to their regional nodal groups, but, with further progression of disease, the complex patterns of interconnections between nodal chains may lead to secondary sites of involvement. Familiarity with these preferential pathways of dissemination will allow the radiologist to specifically evaluate those areas most likely to be involved by a given malignant disease. When the primary lesion is not known, the pattern of nodal involvement may direct further diagnostic studies to the proper organ.

Esophageal and gastric carcinomas primarily spread to the celiac, gastrohepatic ligament, and perisplenic nodes. Later, involvement of the portal and pancreaticoduodenal nodal groups may be seen. Malignant processes of the liver and biliary tree first involve the portal nodes but may spread centrally via extensive interconnections to the celiac axis group. The pancreas is drained by multiple communicating nodal chains, including the perisplenic, pancreaticoduodenal, celiac and superior mesenteric artery, retroperitoneal, and gastrohepatic ligament.

Small bowel malignant processes spread preferentially to the mesenteric nodes and those at the base of the superior mesenteric artery. Carcinomas of the right colon first involve the regional nodes and later spread to the superior mesenteric artery nodes. Carcinomas of the transverse and left colon and rectum also first involve regional nodes; they then spread to the nodes at the base of the inferior mesenteric artery and retroperitoneum. Because they frequently metastasize to the liver, carcinomas of the colon also frequently involve nodes of the porta hepatis.

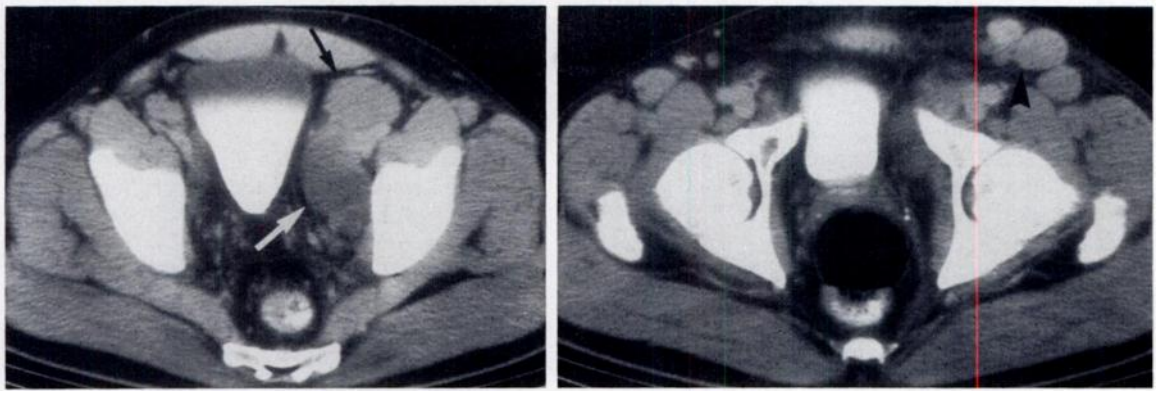

a. b.

Figure 31. CT scans obtained at two different levels in a 46-year-old patient with lymphoma show marked enlargement of the left external iliac (black arrow in **a**), left obturator (white arrow in **a**), and inguinal (arrowhead in **b**) nodes.

Renal and adrenal malignant processes primarily spread to the periaortic retroperitoneal nodes. Carcinomas of the bladder, prostate, cervix, and endometrium initially involve the pelvic nodes but may progress to retroperitoneal nodes. Testicular and ovarian neoplasms initially metastasize to the ipsilateral periaortic nodes at and below the level of the renal hilum. They may then secondarily cross the midline or spread retrograde to the pelvic nodes.

Hodgkin disease tends to follow a logical progression through contiguous nodal chains. Affected nodes tend to be normal in size to only mildly enlarged, and involvement of the mesenteric nodes and viscera is uncommon. In contrast, non-Hodgkin lymphoma has a more random pattern of spread and more commonly involves mesenteric, perivisceral, and extranodal areas. When involved, the nodes tend to be significantly enlarged, often assuming a bulky or confluent appearance.

■ CONCLUSIONS

Many malignant processes cause abdominal lymphadenopathy, and CT has become the primary modality for its detection. The presence of lymphadenopathy has a practical impact on the staging of neoplastic diseases and often dictates the mode of therapy to be used. The effectiveness of therapy can then be followed with serial CT. Knowledge of the CT findings of enlarged lymph nodes in the various nodal chains, the complex series of interconnections between these groups, and the preferential pathways of spread of the major malignant processes is required for accurate interpretation of abdominal lymphadenopathy.

■ REFERENCES

1. Korobkin M. Computed tomography of the retroperitoneal vasculature and lymph nodes. Semin Roentgenol 1981; 16:251–267.
2. Teefey SA, Baron RL, Schulte SJ, Shuman WP. Differentiating pelvic veins and enlarged lymph nodes: optimal CT techniques. Radiology 1990; 175:683–685.
3. Morehouse HT, Thornhill BA. Nodes or no nodes: CT of adenopathy. Crit Rev Diagn Imaging 1985; 25:177–207.
4. Lee JKT. Retroperitoneum. In: Lee JKT, Sagel SS, Stanley RJ, eds. Computed body tomography with MRI correlation. 2nd ed. New York: Raven, 1986; 707–755.
5. Jing B, Wallace S, Zornoza J. Metastases to retroperitoneal and pelvic lymph nodes: computed tomography and lymphangiography. Radiol Clin North Am 1982; 20:511–530.
6. Lee JKT, Stanley RJ, Sagel SS, Levitt RG. Accuracy of computed tomography in detecting intra-abdominal and pelvic adenopathy in lymphoma. AJR 1978; 131:311–315.
7. Walsh JW, Amendola MA, Konderding KF, Tisnado J, Hazra TA. Computed tomographic detection of pelvic and inguinal lymph node metastases from primary and recurrent pelvic malignant disease. Radiology 1980; 137:157–166.
8. Husband JE. Assessment of retroperitoneal and pelvic lymph node disease. Presented at the 13th Annual Course of the Society of Computed Body Tomography, Palm Springs, Calif, April 2–6, 1990.
9. Dorfman RE, Alpern MB, Gross BH, Sandler MA. CT size criteria for normal lymph nodes in the upper abdomen (abstr). Radiology 1990; 177(P):192.

10. Balfe DM, Mauro MA, Koehler RE, et al. Gastrohepatic ligament: normal and pathologic CT anatomy. Radiology 1984; 150:485–490.
11. Rifkin MD, Ehrlich SM, Marks G. Staging of rectal carcinoma: prospective comparison of endorectal US and CT. Radiology 1989; 170:319–322.
12. Zirinsky K, Auh YH, Rubenstein WA, Kneeland JB, Whalen JP, Kazam E. The portacaval space: CT with MR correlation. Radiology 1985; 156:453–460.
13. Shin MS, Berland LL. Computed tomography of retrocrural spaces: normal, anatomic variants, and pathologic conditions. AJR 1985; 145:81–86.
14. Deutch SJ, Sandler MA, Alpern MB. Abdominal lymphadenopathy in benign diseases: CT detection. Radiology 1987; 163:335–338.
15. Gray H; Williams PL, Warwick R, Dyson M, Bannister LH, eds. Gray's anatomy of the human body. London: Churchill Livingstone, 1989; 821–858.
16. Baker ME, Silverman PM, Halvorsen RA Jr, Cohan RH. Computed tomography of masses in periportal/hepatoduodenal ligament. J Comput Assist Tomogr 1987; 11:258–263.
17. Weinstein JB, Heiken JP, Lee JKT, et al. High-resolution CT of the porta hepatis and hepatoduodenal ligament. RadioGraphics 1986; 6:55–74.
18. Zeman RK, Schiebler M, Clark LR, et al. The clinical and imaging spectrum of pancreaticoduodenal lymph node enlargement. AJR 1985; 144:1223–1227.
19. Whitley NO, Bohlman ME, Baker LP. CT patterns of mesenteric disease. J Comput Assist Tomogr 1982; 6:490–496.
20. Silverman PM, Baker ME, Cooper C, Kelvin FM. Computed tomography of mesenteric disease. RadioGraphics 1987; 7:309–320.
21. Mueller PR, Ferrucci JT Jr, Harbin WP, Kirkpatrick RH, Simeone JF, Wittenberg J. Appearance of lymphomatous involvement of the mesentery by ultrasonography and body computed tomography: the "sandwich sign." Radiology 1980; 134:467–473.